electronics

MDPI

Article

Task-Space Cooperative Tracking Control for Networked Uncalibrated Multiple Euler–Lagrange Systems

Zhuoqun Zhao [1,2], Jiang Wang [1] and Hui Zhao [3,*]

[1] School of Electrical and Information Engineering, Tianjin University, Tianjin 300072, China
[2] School of Mechanical Engineering, Tianjin Sino-German University of Applied Sciences, Tianjin 300350, China
[3] School of Electrical Engineering and Automation, Tianjin University of Technology, Tianjin 300384, China
* Correspondence: zhaohui@email.tjut.edu.cn

Abstract: Task-space cooperative tracking control of the networked multiple Euler–Lagrange systems is studied in this paper. On the basis of establishing kinematic and dynamic modeling of a Euler–Lagrange system, an innovative task-space coordination controller is designed to deal with the time-varying communicating delays and uncertainties. First, in order to weaken the influence of the uncertainty of kinematic and dynamic parameters on the control error of the system, the product of the Jacobian matrix and the generalized spatial velocity are linearly parameterized; thus, the unknown parameters are separated from known parameters. The online estimation of uncertain parameters is realized by designing parameters and by proposing new adaptive laws for the dynamic and kinematic parameters. Furthermore, to describe the transmission of time-varying delay errors among networked agents, a new error term is introduced, obtained by adding the observation error and tracking error, and the coefficient of the network mutual coupling term related to the time-varying delay rate is added with reference to the generalized space velocity and task-space velocity of the Lagrange systems. In the end, the influence of the time-varying delay on the cooperative tracking control error of the networked multiple Euler–Lagrange systems is eliminated. With the help of Lyapunov stability theory, the tracking errors and synchronization errors of this system are calculated by introducing the Lyapunov–Krasovskii functional; the asymptotic convergence results rigorously prove the stability of the adaptive cooperative control systems. The simulation results verify the excellent performance of the controller.

Keywords: cooperative tracking control; parameter adaptive law; time-varying delay; networked multiple Euler–Lagrange systems; task-space velocity

Citation: Zhao, Z.; Wang, J.; Zhao, H. Task-Space Cooperative Tracking Control for Networked Uncalibrated Multiple Euler–Lagrange Systems. *Electronics* **2022**, *11*, 2449. https://doi.org/10.3390/electronics11152449

Academic Editor: Juan M. Corchado

Received: 23 June 2022
Accepted: 2 August 2022
Published: 6 August 2022

1. Introduction

With the rapid development of mobile internet technology, multiagent systems found applications in many fields, such as unmanned aerial vehicle swarm [1], sensor network [2], data fusion [3], multi-manipulator systems [4], parallel computing [5], multi-robot systems [6], traffic vehicle clusters [7], and network resource allocation [8]. Generally, the dynamic performance of these systems is described by the Lagrange equation, and they are collectively referred to as Euler–Lagrange systems [9]. To cooperatively accomplish an overall task, efficient teamwork among multiple agents is required. Therefore, team control of multiagent systems has become a hot research topic.

In the last few years, research hotspots related to networked Euler–Lagrange systems mainly involved consistency (cooperative) research [10], formation control [11], and flocking motion control [12]. In addition, the control problem under different network topologies also received great attention [13], such as directed graphs, undirected graphs, and switching topology.

In recent years, scenarios that require multiple agents to cooperate to complete a certain overall control task continued to emerge. In [9], distributed finite-time coordination

control for networked Euler–Lagrange systems under directed graphs was studied. In order to achieve the desired cooperative control goal in limited time, distributed synchronous control and the distributed inclusive control were adopted simultaneously, and the results were verified by simulation. The authors of [14] addressed a robust, adaptive finite-time tracking control scheme for Euler–Lagrange systems. First, the scheme used a Gaussian error function to approximate the input saturation non-linearity, and then the lumped uncertainty term caused by uncertain model parameters and external disturbances was expressed in a linear parametric form with a single parameter. Finally, a new robust adaptive tracking control law was designed to solve the tracking control problem of uncertain Euler–Lagrange systems. Simulation results demonstrate that the proposed control scheme has finite-time convergence speed, as well as robustness to uncertainties and unknown disturbances. Huang Yi et al. [15] studied the problem of fully distributed event-triggered optimal coordinated control for multiple Euler–Lagrange systems. In order to achieve the goal of minimizing the global cost function in a distributed manner, this study introduces a new auxiliary system as a reference model when the model parameters of the Euler–Lagrange system are unknown. Its output converges exponentially to the optimal solution of the global cost function.

With the continuous progress of computer image processing technology, cooperative control gradually transferred from the configuration space to the task space, while visual servo control attracted more and more attention, and the design of visual servo controllers defined in the task space became a research hotspot in this field [16–19]. In the task space, homogeneous transformation is often required when designing a controller according to the system's kinematic and dynamic model. Unfortunately, in many real industrial environments, these dynamic and kinematic parameters can be difficult to obtain or can exhibit uncertainty. However, cooperative control is an effective method to deal with these uncertainties. The authors of [20] proposed a new adaptive synchronous control (ASC) scheme for the uncertainties of the system model of a cable-driven parallel robot (CDPR) and the problems of multicable coordination. In addition to the tracking error, a new synchronization error was introduced to describe the coordinated motion relationship between adjacent cables. The adaptive rates were designed according to the linear expressions of kinematic and dynamic models. Simulation results show that the proposed scheme simultaneously suppresses the uncertainty of kinematics and dynamics, adjusts the coordinated motion of multiple cables, and completes the high-precision tracking task. The authors of [21] studied the tracking problem of a class of heterogeneous linear minimum-phase discrete-time multiagent systems (MASs). By introducing distributed adaptive observers and reference models, the complex cooperative tracking problem of an unknown heterogeneous MAS was transformed into a reference model-to-leader cooperative tracking problem and a locally robust model reference adaptive control problem. Simulation results show that the tracking errors between the outputs of all agents and the leader's output converge to a residual set under the designed adaptive controller. The authors of [22] proposed a hierarchical distributed control scheme, based on local and global information, to achieve the optimal solution of the team objective function, which was used to solve the optimal consistency problem of a group of integrator systems with dynamic uncertainty. The scheme designed an optimal control law based on the neighbor information and local cost function gradient for each agent, and a compensator was derived using the Lyapunov redesign technique to deal with dynamic uncertainties. At the same time, the optimal controller was strengthened by introducing the state difference between neighbors into the compensator. Simulation results show that this scheme ensures the asymptotic convergence of the system in the sense of stability.

In reality, if communication links are unreliable, or the bandwidth is limited, communication flows are, inevitably, delayed. Thus, the communication delay has an important effect on the consistency and synchronization of multiple Euler–Lagrange systems. The authors of [23] proposed a framework for designing robust controllers for a class of nonlinear-networked control systems using non-periodic feedback information. In order to

solve the uncertainty problem in system dynamics, a linear robust control law was derived using optimal control theory, and two different closed-loop systems were considered. In order to save the network bandwidth, the state and input information was transmitted periodically in the feedback loop, the event-triggered control technology was adopted to reduce the transmission cost, and two different event-triggered robust control laws were derived to stabilize the uncertain nonlinear system. The simulation results show that the designed event-triggering controller satisfies the tradeoff between control performance and network bandwidth saving in the case of uncertainty. The authors of [24] studied the network control system used for remote control and monitoring of large complex systems, and they proposed a method of real-time detection and estimation of delayed switching attack, based on Lyapunov theory. A secure control strategy was designed to reduce the influence of delayed switching attack in real time and the influence of network delay on communication between agents. The stability of the secure control system was studied using Lyapunov theory. The performance and security control strategy of the proposed delay switching attack estimator were evaluated using simulations and semi-hardware environments. The authors of [25] studied the distributed tracking control problem of multiple Euler–Lagrange systems with time-varying delays considering full-state constraints and input saturation. First, a distributed observer was designed, such that the follower could obtain the leader's time-varying information. Then, the barrier Lyapunov function technique was used to enable the system error to converge to a certain range, and the influence of control input saturation was overcome using the inverse winding method. Numerical simulation results verify the effectiveness of the algorithm. The authors of [26] studied the consistency of topological interaction groups under communication constraints and time delays. In the case of low noise, a sufficient condition for the stability of the consensus process was given. In addition, this paper also analyzes more complex cases, where noise and finite data rates worked together, revealing that the consensus process is degraded when the data rate is reduced.

From the above analysis, it can be seen that the following problems need to be solved in networked Euler–Lagrange systems: uncertainty in dynamics and kinematics, time-varying communication delays, and the measurement of the task-space velocity. When these problems are coupled, designing a suitable controller to realize cooperative synchronization of multiple agents is difficult. This paper mainly contributes to the literature as follows: (1) a cooperative tracking controller is designed for networked, uncalibrated multiple Euler–Lagrange systems with a strongly connected communication graph; (2) task-space synchronization control considering time-varying communication delay is studied; (3) the coupling effects of uncertainty, time-varying communication delay, and task-space velocity are considered.

2. Research Foundation

Lemma 1 (Barbalat Lemma) [27]. *Suppose* $\varnothing : [0, \infty) \to R$ *is a uniformly continuous function, and* $\lim_{t\to\infty} \int_0^t \varnothing(\tau)d\tau$ *exists and is finite; then, there is* $\varnothing(t) \to 0$ *when* $t \to \infty$.

Lemma 2 [27]. *When the following conditions are true, if* $t \to \infty$, *then the function* $V(x,t) \to 0$:

1. *The lower bound of V(x, t) exists;*
2. $\dot{V}(x,t)$*is negative semi-definite;*
3. $\dot{V}(x,t)$ *is bounded.*

2.1. Algebraic Graph Theory

When there is a directed path between any two vertices of a graph, the network topology is strongly connected.

In this paper, the network was composed of N Euler–Lagrange systems, and its topology was a directed digraph with strong connections. A directed graph is represented by the notation $G(V, E)$, where V denotes non-empty vertex sets representing the nodes in the

network, and $E \in V \times V$ denotes the edge set describing the signal communication between the nodes of the directed graph. In addition, the edge (i, j) represents the communication path from j to i. When there is a directed path between any two vertices of a graph, the network topology is strongly connected [28]. The set of neighbor nodes of the i-th node can be represented by $N_i = \{j|(i, j) \in E\}$. Matrix $W = [w_{ij}]$ represents the weight applied to the directed paths. Here, $if\ j \in N_i$, then $w_{ij} > 0$; otherwise, $w_{ij} = 0$. We assume that one node only transmits the state signals to nodes other than itself (i.e., $i \notin N_i$). Therefore, *if* $i \in V$, then $w_{ij} = 0$. The Laplacian matrix $L = [l_{ij}]$ can be defined as follows:

$$l_{ij} = \begin{cases} \sum\limits_{j \in N_i} w_{ij}\ i = j \\ -w_{ij}\ i \neq j \end{cases} \tag{1}$$

For a strongly connected network, L satisfies Lemma 3.

Lemma 3. *If the Laplace matrix of a strongly connected topological network is L, then there exists a positive vector* $\gamma = [\gamma_{ij,1}, \gamma_{ij,2}, \ldots, \gamma_{ij,N}]^T (\gamma_i > 0\ \forall i \in \{1, \ldots, N\}$ *),which makes the following formula true:*

$$\gamma^T L = 0 \tag{2}$$

2.2. Modeling of Euler–Lagrange Systems

A multiple Euler–Lagrange system includes N Euler–Lagrange subsystems. $x_i(t) \in R^m (i = 1, \ldots, N)$ represents the task-space position vector of the i-th subsystem, where m represents the dimensions of the position coordinate. On the basis of the kinematic characteristics of the Euler–Lagrange subsystem, the task-space position $x_i(t)$ satisfies

$$x_i(t) = f_i(q_i(t)) \tag{3}$$

where $q_i(t) \in R^n$ represents the generalized coordinate position vector of the i-th Lagrange subsystem, n represents the generalized coordinate dimension, and $f_i(*)$ represents the non-linear mapping from the generalized coordinate position to the task-space position, which satisfies

$$f_i(q_i(t)) = \begin{pmatrix} \mathrm{R} & \mathrm{P} \\ 0 & 1 \end{pmatrix} q_i(t) \tag{4}$$

where R is the rotation matrix, and P is the translation vector.

Differentiating Equation (3) yields the task-space velocity [29].

$$\dot{x}_i = J_i(q_i(t))\dot{q}_i(t) \tag{5}$$

where $J_i(q_i(t))$ represents the relation between the generalized coordinate space velocities and task-space velocities of the i-th Euler–Lagrange subsystem, and it describes the kinematic properties.

A Euler–Lagrange system generally has multiple degrees of freedom, e.g., the joint angle dimension of a manipulator. The generalized coordinate space is its joint angle space. It is noteworthy that the kinematic relationships become more and more complex with the increase in dimensions. These complex kinematic relations are included in the Jacobian matrix expressed macroscopically. In fact, the Jacobian matrix has the properties described below [29].

Property 1: The kinematic equation (Equation (5)) is linearly parameterized and the following form is obtained:

$$J_i(q_i(t))\dot{q}_i(t) = Y_{k,i}\big(q_i(t), \dot{q}_i(t)\big)\theta_{k,i} \tag{6}$$

where $Y_{k,i}(q_i(t), \dot{q}_i(t))$ denotes the kinematic regression matrix, and $\theta_{k.i}$ denotes the unknown kinematic parameter vector, which is constant.

For ease of expression, we abbreviate $q_i(t)$ to q_i and $J_i(q_i(t))$ to J_i. Furthermore, according to the Euler–Lagrange Equations (2)–(7), the dynamic equation of the i-th subsystem can be obtained as follows:

$$H_i(q_i)\ddot{q}_i + \left[\frac{1}{2}\dot{H}_i(q_i) + C_i(q_i, \dot{q}_i)\right]\dot{q}_i + g_i(q_i) = \tau_i \tag{7}$$

where $\tau_i \epsilon R^{n\times 1}$ represents the control input vectors of the i-th Euler–Lagrange subsystem (e.g., the joint torque input for the i-th manipulator), $H_i(q_i) \in R^{n\times n}$ represents the symmetric positive definite inertia matrix, $\frac{1}{2}\dot{H}_i(q_i) + C_i(q_i, \dot{q}_i)$ is the Coriolis and centrifugal matrix, $C_i(q_i, \dot{q}_i)$ is the skew-symmetric matrix, and $g_i(q_i)$ represents the gravitational force. Any vector $\Psi \in R^n$ with proper dimensions satisfies

$$\Psi^T C(q(t), \dot{q}(t))\Psi = 0 \tag{8}$$

This property plays a crucial role in the subsequent analysis. Meanwhile, the dynamic equation (Equation (7)) satisfies the property described below.

Property 2: The following equations can be obtained by linearly parameterizing the dynamic Equation (7) of the i-th subsystem.

$$H_i(q_i)\ddot{\xi}_i + \left[\frac{1}{2}\dot{H}_i(q_i) + C_i(q_i, \dot{q}_i)\right]\dot{\xi}_i + g_i(q_i) = Y_{d,i}\left(q_i, \dot{q}_i, \dot{\xi}_i, \ddot{\xi}_i\right)\theta_{d,i} \tag{9}$$

where $\ddot{\xi}_i, \dot{\xi}_i\ R^{\mathrm{n}\times 1}$; $Y_{d,i}\left(q_i, \dot{q}_i, \dot{\xi}_i, \ddot{\xi}_i\right)\ R^{\mathrm{n}\times \mathrm{p3}}$ represents the dynamic regression matrix, and $\theta_{d,i}\ R^{\mathrm{p3}\times 1}$ is the unknown dynamic parameter vector, which is constant. Here, p3 represents the number of unknown parameters, which is related to the dimension of the generalized coordinate vector.

2.3. Description of the Problems and Control Objectives

This paper focuses on networked multiple Euler–Lagrange systems, where the network adopts a strongly connected directed topology, and its switching link between subsystems contains bounded time-varying delay d_{ij} from node j to i. We took the slow time-varying delay communication system as the research object, with a delay change rate $\dot{d}_{ij}$ less than or equal to 1. The kinematic and dynamic parameters ($\theta_{k,i}$ and $\theta_{d,i}$) of Euler–Lagrange systems are usually unknown.

The overall goal of this paper was to realize the asymptotic tracking of the collectively expected task-space trajectory of all Euler–Lagrange subsystems by studying the task-space coordination tracking controller and its control algorithm with excellent performance.

3. Design of Task-Space Cooperative Tracking Controllers

From the above analysis, it can be seen that the Jacobian matrix J_i composed of the kinematic parameters is unknown. In order to solve this problem, our method involves using its estimated matrix $\hat{J}_i$ to design the controller. According to Equation (6), the following formula can be obtained:

$$\hat{J}_i\dot{q}_i = Y_{k,i}(q_i, \dot{q}_i)\hat{\theta}_{k,i} \tag{10}$$

According to Equation (10), the product $\hat{J}_i\dot{q}_i$ consists of two parts: $Y_{k,i}(q_i, \dot{q}_i)$ represents the regression matrix, whereas the parameter vector $\hat{\theta}_{k,i}$ is the estimate of $\theta_{k,i}$, which can be estimated in real time using an adaptive law. On the basis of $\hat{J}_i$, we propose the following observers to estimate the task-space velocity:

$$\dot{\hat{x}}_i(t) = (I + K_{\alpha,i})\hat{J}_i\dot{q}_i + (\beta_i K_{\alpha,i} - \alpha_i I)\widetilde{\Delta x}_i(t) - K_{\alpha,i}\dot{x}_d + 2\beta_i K_{\alpha,i}\Delta x_i(t) \tag{11}$$

where $K_{\alpha,i} = K_{3,i}^{-1}K_{2,i}$; $K_{2,i}$,$K_{3,i}$ denotes the control gain matrices,$\widetilde{\Delta}x_i(t) = \hat{x}_i(t) - x_i(t)$ represents the observation errors, $\Delta x_i(t) = x_i(t) - x_d(t)$ represents the tracking errors, and α, β represent the positive constants.

Furthermore, by differentiating $\widetilde{\Delta}x_i(t) = \hat{x}_i(t) - x_i(t)$, the estimate of the velocity error can be obtained as follows:

$$\begin{aligned}&\widetilde{\Delta}\dot{x}_i(t) = \dot{\hat{x}}_i(t) - \dot{x}_i(t)\\&= K_{\alpha,i}\hat{J}_i(q_i,\dot{q}_i)\dot{q}_i + (\beta_i K_{\alpha,i} - \alpha_i I)\widetilde{\Delta}x_i + Y_{k,i}(q,\dot{q})\Delta\theta_{k,i} - K_{\alpha,i}\dot{x}_d + 2K_\alpha\beta_i\Delta x_i(t)\end{aligned} \tag{12}$$

where $\Delta\theta_{k,i} = \hat{\theta}_{k,i} - \theta_{k,i}$. Furthermore, according to the description of the problem, we need to consider the slow time-varying delay $d_{ij}(t)$ from node j to i, which satisfies the following relationship:

$$\dot{d}_{ij}(t) \le \bar{\dot{d}}_{ij} \le 1 \tag{13}$$

where $\dot{d}_{ij}(t)$ represents the time-varying delay rate, and $\bar{\dot{d}}_{ij}$ represents the upper bound of $\dot{d}_{ij}(t)$. According to the above analysis, the reference generalized space and task-space velocities can be defined as follows:

$$\begin{cases}\dot{x}_{r,i} = \dot{x}_d - \beta_i\Delta\hat{x}_i - \sum\limits_{j\epsilon N_i} w_{ij}\left[\gamma_{ij,1}\Delta\hat{x}_i - \gamma_{ij,2}\overline{\Delta}\hat{x}_j\right]\\ \dot{q}_{r,i} = \hat{J}_i^{+}(q_i)\dot{x}_{r,t}\\ \gamma_{ij,1} = 1 - \frac{\bar{\dot{d}}_{ij}}{2}, \gamma_{ij,2} = 1 - \bar{\dot{d}}_{ij}\end{cases} \tag{14}$$

where $\hat{J}_i^{+}(q_i)$ denotes the pseudo-inverse of $\hat{J}_i(q_i)$, $\overline{\Delta}\hat{x}_j$ is abbreviation of $\Delta\hat{x}_j\left[t - d_{ij}(t)\right] = \hat{x}_j\left[t - d_{ij}(t)\right] - x_d\left[t - d_{ij}(t)\right]$, $\gamma_{ij,1}, \gamma_{ij,2}$ are the gain coefficients of the network mutual coupling term related to the time-delay rate, and $\Delta\hat{x}_i(t) = \hat{x}_i(t) - x_d(t)$ is the estimated tracking error.

Note that, in order to guarantee asymptotic convergence in the synchronization error [30], the mutual coupling term is considered in Equation (14). Compared with the literature [31], the reference generalized space velocities and the reference task-space velocities of Euler–Lagrange systems proposed in this paper include the gain coefficients related to $\dot{d}_{ij}(t)$. Its key function is to ensure that the controller achieves good performance in the presence of time-varying delay.

In addition, differentiating Equation (14) gives the following result:

$$\begin{aligned}\ddot{x}_{r,i} &= \ddot{x}_d - \beta_i\Delta\dot{\hat{x}}_i - \sum_{j\epsilon N_i} w_{ij}\left[\gamma_{ij,1}\Delta\dot{\hat{x}}_i - \gamma_{ij,2}\overline{\Delta}\dot{\hat{x}}_j\right]\\ \ddot{q}_{r,i} &= \dot{\hat{J}}_i^{+}(q_i)\dot{x}_{r,i}(t) + \hat{J}_i^{+}(q_i)\ddot{x}_{r,i}(t)\end{aligned} \tag{15}$$

In the above analysis, a generalized spatial reference velocity was defined in order to carry out stability analysis. Referring to the setup method of the sliding mode vector in [32–34], a generalized spatial velocity sliding mode vector for Euler–Lagrange systems can be defined as follows:

$$S_{q,i} = \dot{q}_i - \dot{q}_{r,i} \tag{16}$$

By comprehensively deriving Equations (10)–(16), the following formula can be obtained:

$$\hat{J}_i S_{q,i} = \Delta\dot{x}_i + \beta_i\Delta\hat{x}_i + Y_{k,i}(q_i,\dot{q}_i)\Delta\theta_{k,i} + \sum_{j\in N_i} w_{ij}\left[\gamma_{ij,1}\Delta\hat{x}_i - \gamma_{ij,2}\overline{\Delta}\hat{x}_j\right] \tag{17}$$

where $\Delta\theta_{k,i}$ represents the estimation error of unknown parameters, $\Delta\theta_{k,i} = \hat{\theta}_{k,i} - \theta_{k,i}$.

By introducing Equation (17) into Equation (11), the following formula can be obtained:

$$\begin{aligned}\widetilde{\Delta}\dot{x}_i(t) = Y_{k,i}(q_i,\dot{q}_i)\Delta\theta_{k,i} - \alpha_i\widetilde{\Delta}x_i + K_{\alpha,i}\hat{J}_i S_{q,i} + K_{\alpha,i}\beta_i\Delta x_i(t)\\ -K_{\alpha,i}\sum\limits_{j\epsilon N_i} w_{ij}\left[\gamma_{ij,1}\Delta\hat{x}_i - \gamma_{ij,2}\overline{\Delta}\hat{x}_j\right]\end{aligned} \tag{18}$$

Above, we analyzed the uncertainty in kinematics; next, we focus on the uncertainty in dynamics. According to Property 2, we can also estimate the dynamic parameters by following a similar method to that used for estimating the kinematic parameters.

$$\hat{H}_i(q_i)\ddot{q}_i + \left[\frac{1}{2}\dot{\hat{H}}_i(q_i) + \hat{C}_i(q_i,\dot{q}_i)\right]\dot{q}_i + \hat{g}_i(q_i) = Y_{d,i}(q_i,\dot{q}_i,\ddot{q}_i)\hat{\theta}_{d,i} \tag{19}$$

where $\hat{\theta}_{d,i}$ represents the estimation vectors of unknown dynamic parameters, and $\hat{H}_i(q_i), \hat{C}_i(q_i,\dot{q}_i), \hat{g}_i(q_i)$ represents the estimation of the corresponding matrices and vectors of dynamic equations.

Our proposed cooperative controller is shown below.

$$\tau_i = Y_{d,i}\left(q_i,\dot{q}_i,\dot{q}_{r,i},\ddot{q}_{r,i}\right)\hat{\theta}_{d,i} - K_{1,i}S_{q,i} - \hat{J}_i^T K_{2,i}\Delta\hat{x}_i(t) \tag{20}$$

where $K_{1,i}$, $K_{2,i}$ are control gain matrices of the i-th Euler–Lagrange subsystem. The block diagram of the cooperative controller is shown in Figure 1.

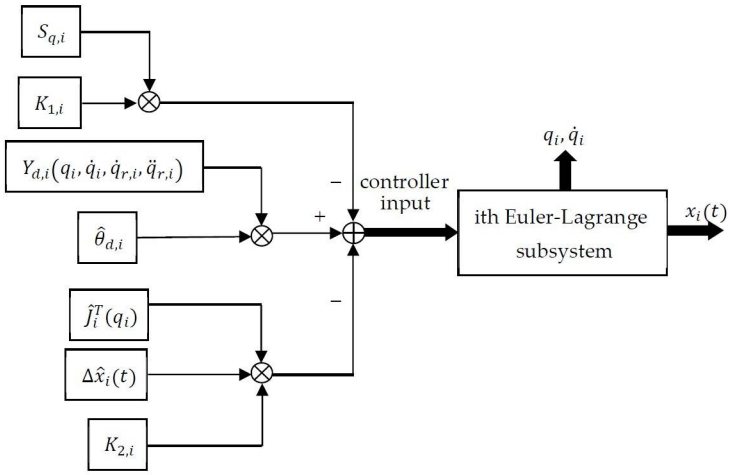

Figure 1. Block diagram of the cooperative controller.

After substituting Equation (20) into Equation (7), the following equation can be obtained:

$$H_i\ddot{q}_i + \left[\frac{1}{2}\dot{H}_i + C_i\right]\dot{q}_i + g_i(q_i) = Y_{d,i}\hat{\theta}_{d,i} - K_{1,i}S_{q,i} - \hat{J}_i^T K_{2,i}\Delta\hat{x}_i(t)$$

By adding the term $(-Y_{d,i}\theta_{d,i})$ to the two sides of the above equation, we obtain the following equation:

$$H_i\ddot{q}_i + \left[\frac{1}{2}\dot{H}_i + C_i\right]\dot{q}_i - Y_{d,i}\theta_{d,i} + g_i(q_i) = Y_{d,i}[\hat{\theta}_{d,i} - \theta_{d,i}] - K_{1,i}S_{q,i} - \hat{J}_i^T K_{2,i}\Delta\hat{x}_i(t)$$

Since $\Delta\theta_{d,i} = \hat{\theta}_{d,i} - \theta_{d,i}$, the following formula holds:

$$H_i\ddot{q}_i + \left[\frac{1}{2}\dot{H}_i + C_i\right]\dot{q}_i - Y_{d,i}\theta_{d,i} + g_i(q_i) = Y_{d,i}\Delta\theta_{d,i} - K_{1,i}S_{q,i} - \hat{J}_i^T K_{2,i}\Delta\hat{x}_i(t)$$

Substituting Equation (16) into the above equation, the following equation can be obtained:

$$\begin{aligned} H_i\dot{S}_{q,i} + \left[\tfrac{1}{2}\dot{H}_i + C_i\right]S_{q,i} + H_i\ddot{q}_{r,i} + \left[\tfrac{1}{2}\dot{H}_i + C_i\right]\dot{q}_{r,i} + g_i(q_i) - Y_{d,i}\Delta\theta_{d,i} \\ = Y_{d,i}\Delta\theta_{d,i} - K_{1,i}S_{q,i} - \hat{J}_i^T K_{2,i}\Delta\hat{x}_i(t) \end{aligned}$$

After substituting Equation (9) into the above equation, the closed-loop system is given by Equation (21).

$$H_i\dot{S}_{q,i} + \left[\frac{1}{2}\dot{H}_i + C_i\right]S_{q,i} = Y_{d,i}\Delta\theta_{d,i} - K_{1,i}S_{q,i} - \hat{j}_i^T K_{2,i}\Delta\hat{x}_i \tag{21}$$

where we abbreviate $H_i(q_i)$ as H_i, $C_i(q_i,\dot{q}_i)$ as C_i and $Y_{d,i}\left(q_i,\dot{q}_i,\dot{q}_{r,i},\ddot{q}_{r,i}\right)$ as $Y_{d,i}$; $\Delta\theta_{d,i} = \hat{\theta}_{d,i} - \theta_{d,i}$ is the estimation error of unknown dynamic parameter vectors.

We propose the adaptive laws for $\theta_{k,i}$ and $\theta_{d,i}$ as follows:

$$\dot{\hat{\theta}}_{d,i} = -\Gamma_{d,i}^{-1}Y_{d,i}^T\left(q_i,\dot{q}_i,\dot{q}_{r,i},\ddot{q}_{r,i}\right)S_{q,i} \tag{22}$$

$$\dot{\hat{\theta}}_{k,i} = \Gamma_{k,i}^{-1}Y_{k,i}^T(q_i,\dot{q}_i)\left[K_{2,i}\Delta x_i(t) - K_{3,i}\widetilde{\Delta}x_i(t)\right] \tag{23}$$

4. Stability Analysis

In this section, we analyze the asymptotic stability of the multiple Euler–Lagrange systems. For the network Lagrange system, when it has a strong connection communication topology, we hope that the designed controller (Equation (20)) can not only ensure the accuracy of the tracking error and synchronization error, but also ensure asymptotic stability under the cooperation of the adaptive laws (Equations (22) and (23)). Specifically, when $t \to \infty$, $\Delta x_i \to 0, \Delta\dot{x}_i \to 0$ and $(x_i - x_j) \to 0, (\dot{x}_i - \dot{x}_j) \to 0, \forall i,j \in V$, where $d_{ij}(t)$ satisfies Equation (13).

First, we construct a Lyapunov-like positive definite function, as follows:

$$V_i = \frac{1}{2}S_{q,i}^T H_i(q_i)S_{q,i} + \frac{1}{2}\Delta x_i^T K_{2,i}\Delta x_i + \frac{1}{2}\widetilde{\Delta}x_i^T(t)K_{3,i}\widetilde{\Delta}x_i(t) + \frac{1}{2}\Delta\theta_{k,i}^T\Gamma_{k,i}\Delta\theta_{k,i} + \frac{1}{2}\Delta\theta_{d,i}^T\Gamma_{d,i}\Delta\theta_{d,i} \tag{24}$$

After differentiating Equation (24), the following result can be obtained:

$$\dot{V}_i = S_{q,i}^T H_i(q_i)\dot{S}_{q,i} + \Delta x_i^T K_{2,i}\Delta\dot{x}_i + \widetilde{\Delta}x_i^T(t)K_{3,i}\widetilde{\Delta}\dot{x}_i(t) + \Delta\dot{\theta}_{k,i}^T\Gamma_{k,i}\Delta\theta_{k,i} + \Delta\dot{\theta}_{d,i}^T\Gamma_{d,i}\Delta\theta_{d,i} \tag{25}$$

Since $\theta_{d,i}$ and $\theta_{k,i}$ are constants, $\dot{\theta}_{d,i} = 0$, $\dot{\theta}_{k,i} = 0$, $\Delta\dot{\theta}_{k,i} = \dot{\hat{\theta}}_{k,i} - \dot{\theta}_{k,i} = \dot{\hat{\theta}}_{k,i}$, and $\Delta\dot{\theta}_{d,i} = \dot{\hat{\theta}}_{d,i} - \dot{\theta}_{d,i} = \dot{\hat{\theta}}_{d,i}$. By substituting Equations (8), (17), (18), and (21) into Equation (25), the following formula is obtained:

$$\begin{aligned}\dot{V}_i = &-S_{q.i}^T K_{1,i}S_{q,i} - \beta_i\Delta x_i^T K_{2,i}\Delta x_i - \alpha_i\widetilde{\Delta}x_i^T K_{3,i}\widetilde{\Delta}x_i \\ &-\Delta\hat{x}_i^T K_{2,i}\sum_{j\in N_i} w_{ij}\left[\gamma_{ij,1}\Delta\hat{x}_i - \gamma_{ij,2}\overline{\Delta}\hat{x}_j\right]\end{aligned} \tag{26}$$

According to the relationship between $\gamma_{ij,1}$ and $\gamma_{ij,2}$ given by Equation (14), Equation (26) can be rewritten as follows:

$$\dot{V}_i = -S_{q.i}^T K_{1,i}S_{q,i} - \beta_i\Delta x_i^T K_{2,i}\Delta x_i - \alpha_i\widetilde{\Delta}x_i^T K_{3,i}\widetilde{\Delta}x_i - \Delta\hat{x}_i^T K_{2,i}\sum_{j\in N_i} w_{ij}\left[\left(\frac{1}{2} + \frac{\gamma_{ij,2}}{2}\right)\Delta\hat{x}_i - \gamma_{ij,2}\overline{\Delta}\hat{x}_j\right] \tag{27}$$

For networked multiple Lagrange systems, we introduce the following Lyapunov−Krasovskii functional (LKF):

$$\mathrm{V} = \sum_{i=1}^{N}\eta_i^T V_i + \sum_{i=1}^{N}\sum_{j\in N_i}\eta_i^T\frac{w_{ij}}{2}\int_{t-d(t)}^{t}\Delta\hat{x}_j^T(s)K_{2,j}\Delta\hat{x}_j(s)ds \tag{28}$$

By differentiating Equation (28) and substituting Equations (12)–(14) and (21)–(23), the following inequality can be obtained:

$$\begin{aligned}\dot{V} \leq \quad & -\sum_{i=1}^{N}\eta_i^T S_{q,i}^T K_{1,i} S_{q,i} - \sum_{i=1}^{N}\eta_i^T \Delta x_i^T \beta_i k_{2,i} \Delta x_i - \sum_{i=1}^{N}\eta_i^T \alpha_i \widetilde{\Delta} x_i^T K_{3,i} \widetilde{\Delta} x_i \\ & -\sum_{i=1}^{N}\sum_{j\epsilon N_i}\eta_i^T w_{ij} \Delta\hat{x}_i^T K_{2,i}\left[\left(\tfrac{1}{2}+\tfrac{\gamma_{ij,2}}{2}\right)\Delta\hat{x}_i - \gamma_{ij,2}\overline{\Delta}\hat{x}_j\right] \\ & +\sum_{i=1}^{N}\sum_{j\epsilon N_i}\eta_i^T \tfrac{w_{ij}}{2}\left[\Delta\hat{x}_j^T K_{2,j}\Delta\hat{x}_j - \gamma_{ij,2}\overline{\Delta}\hat{x}_j^T K_{2,j}\overline{\Delta}\hat{x}_j\right]\end{aligned} \tag{29}$$

Let $K_{2,i}$=$K_{2,j}$; with the aid of Lemma 2, the following formula is true:

$$\begin{aligned}& -\sum_{i=1}^{N}\sum_{j\in N_i}\eta_i^T \tfrac{w_{ij}}{2}\left[\Delta x_i^T K_{2,i}\Delta x_i - \Delta x_j^T K_{2,j}\Delta x_j\right] = \\ & -\tfrac{\eta_i^T}{2} L\left(\Delta x_1^T K_{2,1}\Delta x_1 \ldots \Delta x_N^T K_{2,N}\Delta x_N\right) = 0.\end{aligned} \tag{30}$$

Therefore, Equation (29) can be arranged as

$$\begin{aligned}\dot{V} \leq & -\sum_{i=1}^{N}\eta_i^T S_{q,i}^T K_{1,i} S_{q,i} - \sum_{i=1}^{N}\eta_i^T \beta_i \Delta x_i^T K_{2,i}\Delta x_i - \sum_{i=1}^{N}\eta_i^T \alpha_i \widetilde{\Delta} x_i^T(t) K_{3,i}\widetilde{\Delta} x_i(t) \\ & -\sum_{i=1}^{N}\sum_{j\in N_i}\eta_i w_{ij}\tfrac{\gamma_{ij,2}}{2}\left[\Delta\hat{x}_i - \overline{\Delta}\hat{x}_j\right]^T K_{2,i}\left[\Delta\hat{x}_i - \overline{\Delta}\hat{x}_j\right]\end{aligned} \tag{31}$$

According to Equations (13) and (14), we have $\dot{\bar{d}}_{ij} \leq 1$, $\gamma_{ij,2} = 1 - \dot{\bar{d}}_{ij} \geq 0$. Then, $\dot{V} \leq 0$ holds, which means that V has an upper bound. Therefore, $S_{q,i}$, $\Delta x_i(t)$, $\widetilde{\Delta} x_i(t)$, $\Delta\theta_{k,i}$, and $\Delta\theta_{d,i}$ are bounded. Hence, $S_{q,i}$, $\Delta x_i(t)$, $\widetilde{\Delta} x_i(t)$, $\Delta\theta_{k,i}$, and $\Delta\theta_{d,i} \in L_2 \cap L_\infty$. From Equations (22) and (23), $\Delta\dot{\theta}_{k,i}, \Delta\dot{\theta}_{d,i} \in L_\infty$ can be derived. Since $\Delta\hat{x}_i(t) = \widetilde{\Delta} x_i(t) + \Delta x_i(t)$, then $\Delta\hat{x}_i(t) \in L_\infty$. Furthermore, from Equation (14), we can conclude that $\dot{x}_{r,t} \in L_\infty, \dot{q}_{r,i} \in L_\infty$. With $S_{q,i} \in L_\infty$, $\dot{q}_i \in L_\infty$ holds; then $\dot{x}_i(t) \in L_\infty, \Delta\dot{x}_i(t) \in L_\infty$ can be easily deduced. Since $\dot{q}_i$, $\widetilde{\Delta} x_i(t)$, $\Delta x_i(t)$ are bounded, we have $\dot{\hat{x}}_i(t) \in L_\infty$ by means of Equation (11). Due to the bounded $\dot{x}_i(t)$, $\widetilde{\Delta}\dot{x}_i(t) \in L_\infty$, it is easy to derive $\ddot{x}_{r,t}(t) \in L_\infty, \ddot{q}_{r,i}(t) \in L_\infty$ using Equation (15). From Equation (21), $\dot{S}_{q,i} \in L_\infty$ exists. By differentiating $\dot{V}$, $\ddot{V} \in L_\infty$ can be derived. Thus, $\ddot{V}$ is bounded. According to Lemma 1, when $t \to \infty$, $\dot{V} \to 0$ exists. Therefore, $\Delta\hat{x}_i - \overline{\Delta}\hat{x}_j \to 0$ for $i \in V, j \in N_i$ as $t \to \infty$.

Furthermore, $\Delta\hat{x}_i - \overline{\Delta}\hat{x}_j$ is convergent, which means that $(\Delta\hat{x}_i - \Delta\hat{x}_j \to 0)$ and $\left(\Delta\hat{x}_j - \overline{\Delta}\hat{x}_j\right) \to 0$, for $i \in V, j \in N_i$ as $t \to \infty$. Similarly, $\dot{x}_i - \dot{x}_j \to 0$ can also be derived. For strongly connected graphs, there exists $x_i - x_j \to 0$, $\dot{x}_i - \dot{x}_j \to 0$ for $i, j \in V$ as $t \to \infty$.

5. Numerical Simulation

To test the performance of the proposed controller, a six-DOF manipulator system in a strongly connected network was taken as an example for simulation. The image plane was considered as the task-space. First, the Laplace matrix L is given as follows:

$$L = \begin{bmatrix} 1 & -0.5 & 0 & -0.2 & 0 & -0.3 \\ 0 & 1 & -1 & 0 & 0 & 0 \\ 0 & -0.5 & 1 & -0.5 & 0 & 0 \\ 0 & -1 & -1 & 3 & 0 & -1 \\ -0.3 & -0.7 & 0 & 0 & 1.5 & -0.5 \\ 0 & 0 & -0.5 & -0.2 & 0 & 0.7 \end{bmatrix} \tag{32}$$

The time-varying delays in network communication topology are defined by the following matrix:

$$= \begin{bmatrix} 0 & x & 0 & z & 0 & m \\ 0 & 0 & y & 0 & 0 & 0 \\ 0 & y & 0 & y & 0 & 0 \\ 0 & x & y & 0 & 0 & m \\ z & x & 0 & 0 & 0 & y \\ 0 & 0 & x & z & 0 & 0 \end{bmatrix} \tag{33}$$

where $x = 0.3 + 0.5\sin(\mathrm{t}/2)$, $y = 0.1 + 0.6\sin(\mathrm{t}/2)$, $z = 0.6 + 0.7\sin(t/2)$, and $\mathrm{m} = 0.4 + 0.4\sin(\mathrm{t}/2)$.

From Equations (13) and (14), $\gamma_{ij,1}$ and $\gamma_{ij,2}$ can be obtained as $\gamma_{12,1} = \gamma_{52,1} = \gamma_{42,1} = \gamma_{63,1} = 0.75$, $\gamma_{32,1} = \gamma_{23,1} = \gamma_{43,1} = \gamma_{34,1} = \gamma_{56,1} = 0.7$, $\gamma_{14,1} = \gamma_{51,1} = \gamma_{64,1} = 0.65$, $\gamma_{16,1} = \gamma_{46,1} = 0.8$, $\gamma_{12,2} = \gamma_{52,2} = \gamma_{42,2} = \gamma_{63,2} = 0.5$, $\gamma_{32,2} = \gamma_{23,2} = \gamma_{43,2} = \gamma_{34,2} = \gamma_{56,2} = 0.4$, and $\gamma_{14,2} = \gamma_{51,2} = \gamma_{64,2} = 0.3$, $\gamma_{16,2} = \gamma_{46,2} = 0.6$.

In this simulation, this paper took the two-link manipulator system as an example to illustrate the problem simply and effectively with the following parameters: connecting rod length, $l_{i,1} = l_{i,2} = 1$ m; distance between the center of gravity of the connecting rod and the first connection, $l_{ci,1} = l_{ci,2} = 0.5$ m; mass, $l_{m,1} = l_{m,2} = 0.5$ kg; length of the object to be grabbed, $l_{o,1} = 0.1$ m. Since each manipulator is the same, their parameters are also the same. The vertex at the end of the grasping object away from the grasping point was chosen as the reference point.

As the actual dynamic parameters are unknown, they are estimated by the linearization method described in Properties 1 and 2. In the simulation process, we randomly set $\theta_{d,i}$ and $\theta_{k,i}$ which represent unknown dynamic and kinematic parameter vectors, respectively; the unknown parameter vectors were updated iteratively in real time through the adaptive law, thus, eventually converging to a constant vector equal to the actual value. The controller gains are $K_{1,i} = 1.35I_2, K_{2,i} = 0.75I_2$, $K_{3,i} = 55I_2, \Gamma_{d,i} = 0.1I_2, \Gamma_{k,i} = I_2$, $\alpha_i = 17, \beta_i = 8$, i = 1,…,6. We chose the common expected trajectory on the image plane to be a circle, where $x_{d,1}(t) = 0.50 + 0.1\sin(0.54 + 3t)$, $x_{d,2}(t) = 0.50 + 0.1\cos(0.54 + 3t)$.

Figures 2–6 show the simulation results, in which the convergence of the position and velocity tracking errors of the six agents on the *X*- and *Y*-axes are shown in Figures 2 and 3, respectively, and the actual positions of the six agents on the *X*- and *Y*-axes are shown in Figure 4. Figure 5 shows the convergence of the *X*-axis synchronization error between the two agents, and Figure 6 shows the convergence of the kinematic parameter estimates when three different initial values are taken. The results show that the estimated values of kinematic parameters gradually converge to their actual values over time without being affected by different initial values.

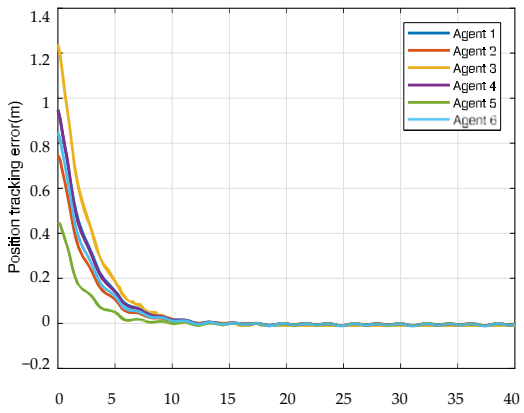

(**a**) Position error curves on *X*-axis

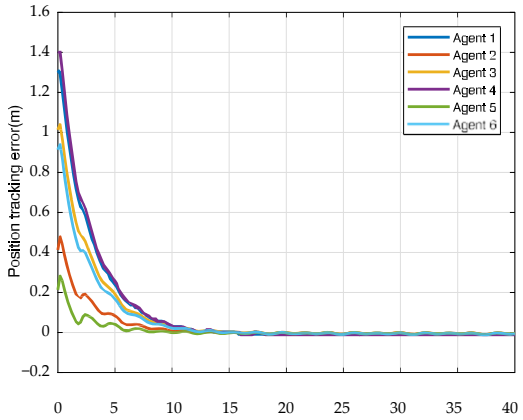

(**b**) Position error curves on *Y*-axis

Figure 2. Position error curves of six agents.

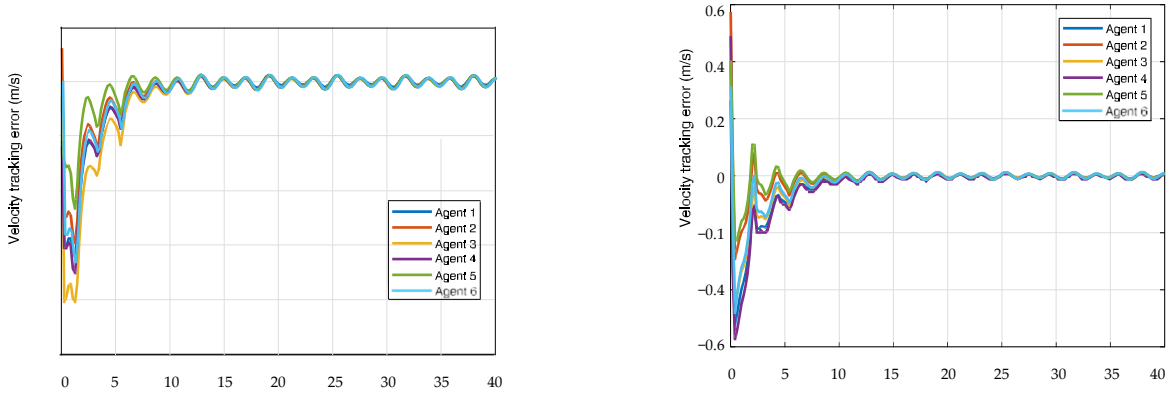

(**a**) Velocity error curves on *X*-axis (**b**) Velocity error curves on *Y*-axis

Figure 3. Velocity error curves of six agents.

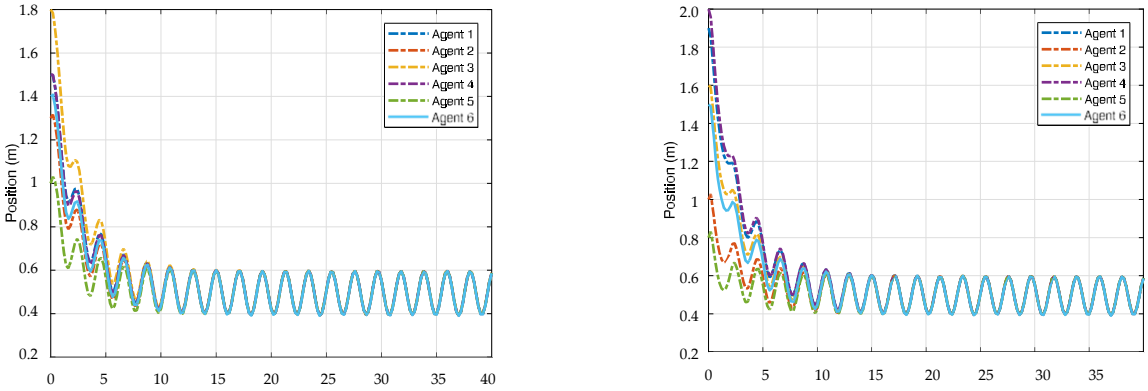

(**a**) Actual position on *X*-axis (**b**) Actual position on *Y*-axis

Figure 4. The actual positions of six agents.

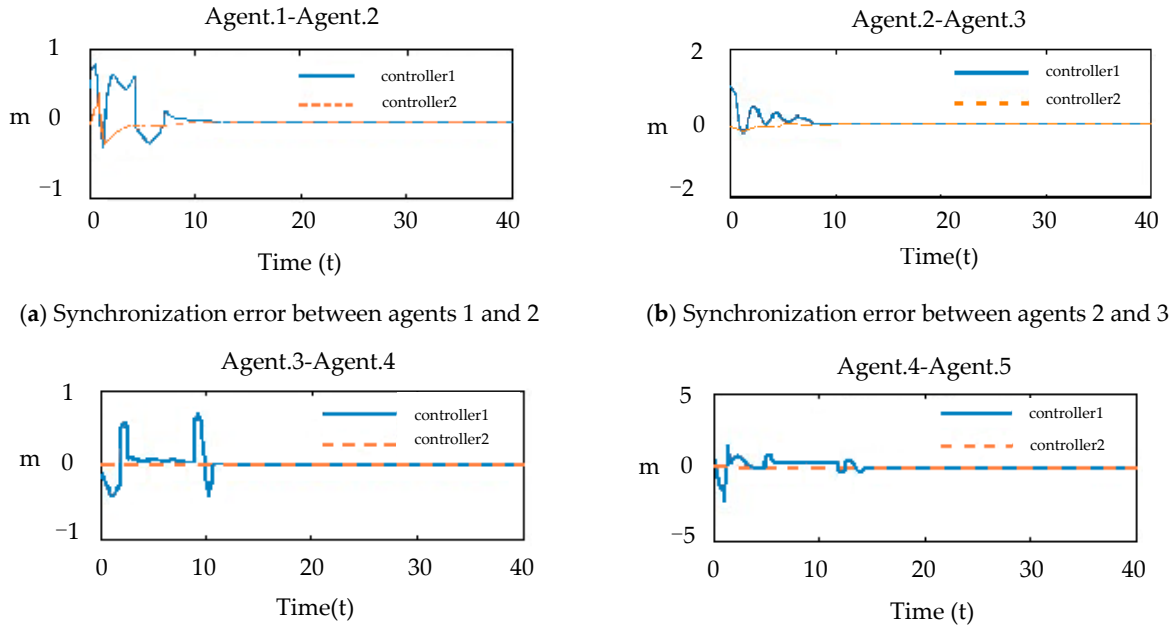

(**a**) Synchronization error between agents 1 and 2 (**b**) Synchronization error between agents 2 and 3

(**c**) Synchronization error between agents 3 and 4 (**d**) Synchronization error between agents 4 and 5

Figure 5. *Cont.*

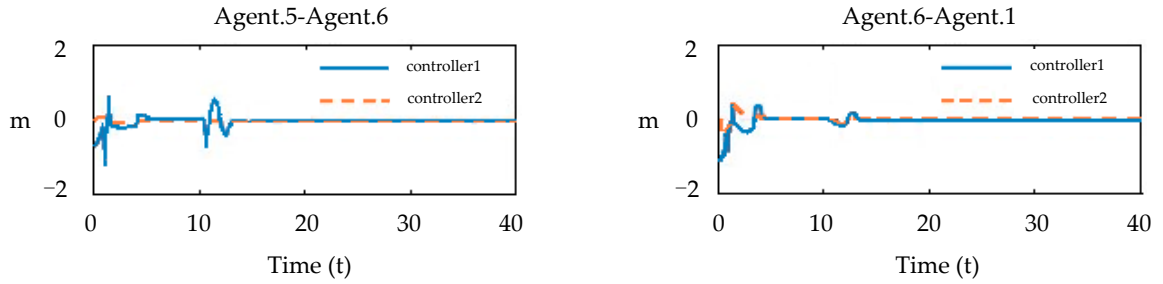

(**e**) Synchronization error between agents 5 and 6 (**f**) Synchronization error between agents 6 and 1

Figure 5. Synchronization error between two agents on *X*-axis.

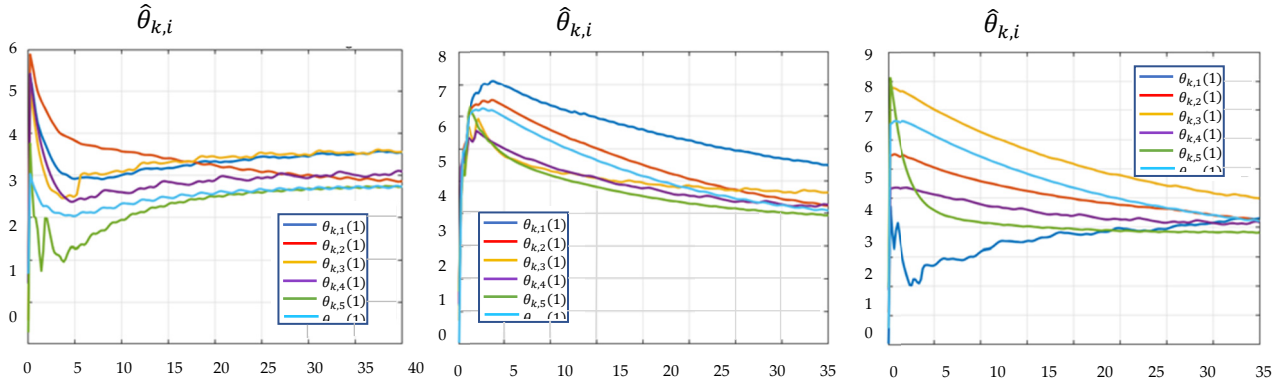

(**a**) (**b**) (**c**)

Figure 6. Kinematic parameter estimates $\hat{\theta}_{k,i}$ when $\hat{\theta}_{k,i}(0)$ has three different initial values. (**a**) $\hat{\theta}_{k,i}(0) = \hat{\theta}_{k,i}(01)$, (**b**) $\hat{\theta}_{k,i}(0) = \hat{\theta}_{k,i}(02)$, (**c**) $\hat{\theta}_{k,i}(0) = \hat{\theta}_{k,i}(03)$.

The research results in this paper were compared with the case in [34], which can only handle constant communication delay. The synchronization error curve is shown in Figure 5. Controller 1 was proposed in [31], whereas controller 2 was proposed in this paper. The simulation results show that the proposed controller (Equation (20)) guarantees the asymptotic convergence of the synchronization error between agents; hence, networked Euler–Lagrange systems with time-varying delays can realize synchronization in the task-space, even in the case of dynamic and kinematic uncertainties.

Note that, when estimating unknown parameters, the variation range of unknown parameters is generally determined on the basis of engineering experience, and the initial value of parameter estimation is selected within this range. In this paper, the initial value of the kinematic parameters of the robotic subsystems was randomly selected within the range [1,3].

6. Conclusions

First, a novel task-space cooperative tracking control strategy was proposed for networked, uncalibrated, multiple Euler–Lagrange systems with complex characteristics, including kinematic, dynamic uncertainty, and time-varying communication delay. By considering the influence of time-varying communication delay, a task-space reference velocity observer was proposed to solve the problem where the task-space velocity is not easy to obtain.

Second, adaptive laws for estimating uncertain kinematic and dynamic parameters were designed. Using these adaptive laws, unknown kinematic and dynamic parameters can be estimated in real time, so as to ensure that the networked, uncalibrated, multiple

Euler–Lagrange system can track a collectively expected trajectory in the presence of time-varying communication delays.

Third, with the help of Lyapunov stability analysis theory, the asymptotic convergence of the tracking error and synchronization error of the system was proven. Simulation results show that the proposed task-space cooperative tracking control strategy has good control performance. This research provides an effective control scheme for the collaborative control of networked robot systems with complex characteristics, and its results lay a foundation for the real-time control of multiagent systems in the future.

Author Contributions: Conceptualization, Z.Z. and J.W.; methodology, H.Z.; software, Z.Z. and H.Z.; validation, Z.Z., J.W., and H.Z.; formal analysis, H.Z.; investigation, J.W.; resources, J.W.; data curation, Z.Z. and H.Z.; writing—original draft preparation, Z.Z.; writing—review and editing, H.Z.; visualization, Z.Z.; supervision, J.W.; project administration, Z.Z.; funding acquisition, H.Z. All authors have read and agreed to the published version of the manuscript.

Funding: This research was funded by the Key Research and Development Projects in Tianjin, grant number 19YFZCSN00360.

Institutional Review Board Statement: The paper does not involve human or animal research.

Informed Consent Statement: The study did not involve humans.

Data Availability Statement: The data that support the findings of this study are included within the article.

Conflicts of Interest: The authors declare no conflict of interest.

References

1. Kang, Y.; Kuang, Y.; Cheng, J.; Zhang, B.; Qi, Y.; Zhou, S.; Mao, K. Robust leaderless time-varying formation control for unmanned aerial vehicle swarm system with Lipschitz nonlinear dynamics and directed switching topologies. *Chin. J. Aeronaut.* **2021**, *35*, 124–136. [CrossRef]
2. Sanjay, K.N.; Shaila, K.; Venugopal, K.R. Designing WiMAX Static Environment using Local Automata based Autonomic Network Architecture for Wireless Sensor Networks. *Procedia Comput. Sci.* **2021**, *184*, 947–952.
3. Stavropoulos, G.; van Vorstenbosch, R.; Jonkers, D.M.; Penders, J.; Hill, J.E.; van Schooten, F.J.; Smolinska, A. Advanced data fusion: Random forest proximities and pseudo-sample principle towards increased prediction accuracy and variable interpretation. *Anal. Chim. Acta* **2021**, *1183*, 339001. [CrossRef]
4. Su, C.; Zhang, S.; Lou, S.; Wang, R.; Cao, G.; Yang, L.; Wang, Q. Trajectory coordination for a cooperative multi-manipulator system and dynamic simulation error analysis. *Robot. Auton. Syst.* **2020**, *131*, 103588. [CrossRef]
5. Benalla, M.; Achchab, B.; Hrimech, H. On the computational complexity of Dempster's Rule of combination, a parallel computing approach. *J. Comput. Sci.* **2021**, *50*, 101283. [CrossRef]
6. He, Y.; Wu, M.; Liu, S. A cooperative optimization strategy for distributed multi-robot manipulation with obstacle avoidance and internal performance maximization. *Mechatronics* **2021**, *76*, 102560. [CrossRef]
7. Pan, T.; Guo, R.; Lam, W.H.; Zhong, R.; Wang, W.; He, B. Integrated optimal control strategies for freeway traffic mixed with connected automated vehicles: A model-based reinforcement learning approach. *Transp. Res. Part C Emerg. Technol.* **2021**, *123*, 102987. [CrossRef]
8. Sharma, N.; Kumar, K. Resource allocation trends for ultra dense networks in 5G and beyond networks: A classification and comprehensive survey. *Phys. Commun.* **2021**, *48*, 101415. [CrossRef]
9. Xu, T.; Lv, Y.; Duan, Z. Distributed Finite-Time Coordination Control for Networked Euler-Lagrange Systems Under Directed Graphs. *IFAC-PapersOnLine* **2020**, *53*, 2453–2458. [CrossRef]
10. Li, S.; Zou, W.; Xiang, Z. Neural-network-based consensus of multiple Euler-Lagrange systems with an event-triggered mechanism. *J. Frankl. Inst.* **2021**, *358*, 8625–8638. [CrossRef]
11. Chen, L.; Li, C.; Xiao, B.; Guo, Y. Formation-containment control of networked Euler–Lagrange systems: An event-triggered framework. *ISA Trans.* **2019**, *86*, 87–97. [CrossRef] [PubMed]
12. Colombo, L.; Moreno, P.; Ye, M.; de Marina, H.G.; Cao, M. Forced variational integrator for distance-based shape control with flocking behavior of multi-agent systems. *IFAC-PapersOnLine* **2020**, *53*, 3348–3353. [CrossRef]
13. Liu, H.; Wang, Y.; Xi, J. Completely distributed formation control for networked quadrotors under switching communication topologies. *Syst. Control. Lett.* **2021**, *147*, 104841. [CrossRef]
14. Chen, C.; Zhu, G.; Zhang, Q.; Zhang, J. Robust adaptive finite-time tracking control for uncertain Euler-Lagrange systems with input saturation. *IEEE Access* **2020**, *8*, 187605–187614. [CrossRef]
15. Huang, Y.; Meng, Z. Fully Distributed Event-Triggered Optimal Coordinated Control for Multiple Euler-Lagrangian Systems. *IEEE Trans. Cybern.* **2021**, *51*, 1–12. [CrossRef] [PubMed]

16. Tsuchida, S.; Lu, H.; Kamiya, T.; Serikawa, S. Characteristics based visual servo for 6DOF robot arm control. *Cogn. Robot.* **2021**, *1*, 76–82. [CrossRef]
17. Ribeiro, E.G.; de Queiroz Mendes, R.; Grassi, V., Jr. Real-time deep learning approach to visual servo control and grasp detection for autonomous robotic manipulation. *Robot. Auton. Syst.* **2021**, *139*, 103757. [CrossRef]
18. Guo, J.; Zhu, Z.; Sun, B.; Zhang, T. A novel field box girder welding robot and realization of all-position welding process based on visual servoing. *J. Manuf. Process.* **2021**, *63*, 70–79. [CrossRef]
19. Zou, J. Predictive visual control framework of mobile robot for solving occlusion. *Neurocomputing* **2021**, *423*, 474–489. [CrossRef]
20. Ji, H.; Shang, W.; Cong, S. Adaptive synchronization control of cable-driven parallel robots with uncertain kinematics and dynamics. *IEEE Trans. Ind. Electron.* **2021**, *68*, 8444–8454. [CrossRef]
21. Yang, R.; Liu, L.; Feng, G. Cooperative Tracking Control of Unknown Discrete-Time Linear Multiagent Systems Subject to Unknown External Disturbances. *IEEE Trans. Cybern.* **2022**, *52*, 1–13. [CrossRef] [PubMed]
22. Guo, G.; Zhang, R. Lyapunov Redesign-Based Optimal Consensus Control for Multi-Agent Systems with Uncertain Dynamics. *IEEE Trans. Circuits Syst. II Express Briefs* **2022**, *69*, 2902–2906. [CrossRef]
23. Tripathy, N.S.; Kar, I.N.; Chamanbaz, M.; Bouffanais, R. Robust stabilization of a class of nonlinear systems via aperiodic sensing and actuation. *IEEE Access* **2020**, *8*, 157403–157417. [CrossRef]
24. Victorio, M.; Sargolzaei, A.; Khalghani, M.R. A Secure Control Design for Networked Control Systems with Linear Dynamics under a Time-Delay Switch Attack. *Electronics* **2021**, *10*, 322. [CrossRef]
25. Sun, Y.; Dong, D.; Qin, H.; Wang, W. Distributed tracking control for multiple Euler–Lagrange systems with communication delays and input saturation. *ISA Trans.* **2020**, *96*, 245–254. [CrossRef]
26. Komareji, M.; Shang, Y.; Bouffanais, R. Consensus in topologically interacting swarms under communication constraints and time-delays. *Nonlinear Dyn.* **2018**, *93*, 1287–1300. [CrossRef]
27. Slotine, J.J.E.; Jean-Jacques, E.; Li, W. *Applied Nonlinear Control*; China Machine Press: Beijing, China; Prentice Hall: Hoboken, NJ, USA, 2004.
28. Godsil, C.; Royle, G. *Algebraic Graph Theory (Graduate Texts in Mathematics)*; Cambridge University Press: Cambridge, UK, 1994; Volume 207.
29. Cheah, C.C.; Liu, C.; Slotine, J.J.E. Adaptive Tracking Control for Robots with Unknown Kinematic and Dynamic Properties. *Int. J. Robot. Res.* **2006**, *25*, 283–296. [CrossRef]
30. Zhai, A.; Wang, J.; Zhang, H.; Lu, G.; Li, H. Adaptive robust synchronized control for cooperative robotic manipulators with uncertain base coordinate system. *ISA Trans.* **2021**, *126*, 134–143. [CrossRef] [PubMed]
31. Liang, X.; Wang, H.; Liu, Y.H.; Chen, W.; Hu, G.; Zhao, J. Adaptive Task-Space Cooperative Tracking Control of Networked Robotic Manipulators Without Task-Space Velocity Measurements. *IEEE Trans. Cybern.* **2016**, *46*, 2386. [CrossRef] [PubMed]
32. Qiu, Z.; Hu, S.; Liang, X. Disturbance observer based adaptive model predictive control for uncalibrated visual servoing in constrained environments. *ISA Trans.* **2020**, *106*, 40–50. [CrossRef]
33. Ren, X.; Li, H. Uncalibrated Image-Based Visual Servoing Control with Maximum Correntropy Kalman Filter. *IFAC-PapersOnLine* **2020**, *53*, 560–565.
34. Liu, X.; Mao, J.; Yang, J.; Li, S.; Yang, K. Robust predictive visual servoing control for an inertially stabilized platform with uncertain kinematics. *ISA Trans.* **2021**, *114*, 347–358. [CrossRef] [PubMed]